Photosynthetic electron partitioning between [FeFe]-hydrogenase and ferredoxin:NADP$^+$-oxidoreductase (FNR) enzymes in vitro

Iftach Yacoby[a,1], Sergii Pochekailov[a], Hila Toporik[b], Maria L. Ghirardi[c], Paul W. King[c,1], and Shuguang Zhang[a,1]

[a]Center for Biomedical Engineering NE47-379, Massachusetts Institute of Technology, 77 Massachusetts Avenue, Cambridge, MA 02139-4307; [c]Biosciences Center, National Renewable Energy Laboratory, 1617 Cole Boulevard, Golden, CO 80401-3305; and [b]Department of Biochemistry and Molecular Biology, The George S. Wise Faculty of Life Sciences, Tel Aviv University, Tel Aviv, 69978, Israel

Photosynthetic water splitting, coupled to hydrogenase-catalyzed hydrogen production, is considered a promising clean, renewable source of energy. It is widely accepted that the oxygen sensitivity of hydrogen production, combined with competition between hydrogenases and NADPH-dependent carbon dioxide fixation are the main limitations for its commercialization. Here we provide evidence that, under the anaerobic conditions that support hydrogen production, there is a significant loss of photosynthetic electrons toward NADPH production in vitro. To elucidate the basis for competition, we bioengineered a ferredoxin-hydrogenase fusion and characterized hydrogen production kinetics in the presence of Fd, ferredoxin:NADP$^+$-oxidoreductase (FNR), and NADP$^+$. Replacing the hydrogenase with a ferredoxin-hydrogenase fusion switched the bias of electron transfer from FNR to hydrogenase and resulted in an increased rate of hydrogen photoproduction. These results suggest a new direction for improvement of biohydrogen production and a means to further resolve the mechanisms that control partitioning of photosynthetic electron transport.

Photosynthetic hydrogen production has been known for over 70 years (1). Many microalgae and cyanobacteria are able to anaerobically express hydrogenase enzymes that reduce protons to gaseous hydrogen. This process, however, is limited to strict anaerobic growth conditions. Algal [FeFe]-hydrogenases (HydA) generate hydrogen through the oxidation of reduced ferredoxin (Fd), an electron mediator that is initially reduced by photosystem I (PSI) (2–4). However, besides providing reductant for hydrogen production, Fd is the main electron donor to many metabolic pathways, including production of NADPH for carbon dioxide fixation, nitrate reduction, cyclic electron flow (CEF), nitrite and sulfite reduction, and other reductive reactions (5, 6). Central questions in the study of photobiological hydrogen production are the following: (*i*) What controls the partitioning of electrons between competing metabolic pathways? (*ii*) What mechanisms mediate this control under anaerobic, hydrogen-producing conditions? (*iii*) Are these mechanisms operational under aerobic conditions if an oxygen-tolerant hydrogenase becomes available? These questions are particularly important if photosynthetic hydrogen production is to become a feasible fuel source, because it has the potential to generate inexhaustible renewable energy through splitting of water.

In this systematic study, we focused on two major reactions that depend on reduced ferredoxin: (*i*) hydrogen production, catalyzed by HydA, and (*ii*) NADPH production catalyzed by the enzyme ferredoxin:NADP$^+$-oxidoreductase (FNR) (6). Under aerobic conditions, HydA enzyme expression is suppressed, and NADPH production dominates. A continuous NADPH supply is a prerequisite for carbon dioxide fixation and is produced by photosynthetic linear electron flow (LEF) (Fig. 1*A*). Both reduced Fd and NADPH have been proposed to act as electron mediators in the buildup of a proton gradient through CEF (Fig. 1*B*). The partitioning of photosynthetic reductant between
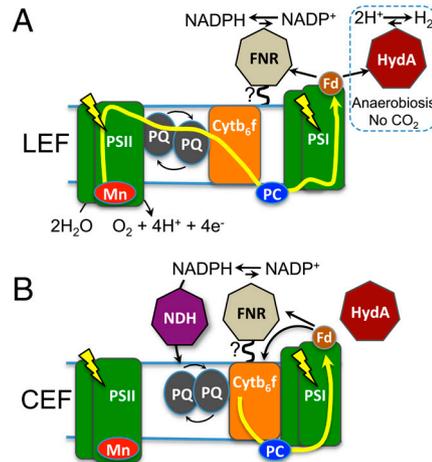

Fig. 1. *Photosynthetic electron transport pathways that support the production of NADPH and hydrogen.* (*A*) In LEF, light-activated PSII extracts electrons from water and transfers them in a Z-scheme pattern to plastoquinone (PQ), then, through Cytochrome b_6f, ($Cytb_6f$) to PC, which then feeds electrons to light-oxidized PSI. PSI-derived electrons are used to reduce Fd, which then transfers reductant to either FNR, for NADPH production, or to HydA, for hydrogen production. During aerobic LEF, hydrogen production is absent due to (*i*) oxygen formation by PSII and (*ii*) NADPH-dependent carbon dioxide assimilation mediated by FNR. In the figure, FNR is shown associated with the thylakoid membrane, as proposed by previous studies (see text) and also confirmed here. LEF can support hydrogen production only during anaerobic growth, when oxygen is either removed by argon purging or consumed by respiration (see text). (*B*) During CEF, electrons are cycled around PSI, which supports generation of a proton gradient. Electrons originating from Fd are either transferred to Cyb6f or to FNR to produce NADPH, which is consumed by NADPH dehydrognease to reduce the PQ pool. Presumably HydA is unable to compete (or competes weakly) with CEF mechanism(s) during anaerobic growth.

carbon dioxide fixation and CEF is regulated by many physiological factors (7–9) and mostly depends on the requirement of the organism for ATP vs. NADPH.

Activation of alternative electron sinks such as hydrogen production (7, 9) can be initiated under anaerobic growth and in combination with nutrient limiting conditions. Such conditions,

i.e., argon or helium purging or sulfur-deprivation conditions (10), can totally or partially suppress carbon dioxide fixation (9, 10). The rates of hydrogen production measured under anaerobiosis reflect the inherent low conversion efficiencies (11), which are partly due to competition with carbon dioxide fixation, CEF and the buildup of a proton gradient. This is evidenced by the increased rates of hydrogen production in the presence of proton uncouplers (12), in an *stm-6* mutant (8) that has diminished CEF, and in a Rubisco mutant (7) that cannot fix carbon dioxide. Thus, attaining efficient conversion of solar energy into hydrogen in atmospheric conditions (with an oxygen-tolerant hydrogenase) will require developing a mechanistic understanding of how the cell controls reductant fluxes among these various metabolic pathways. Based on this knowledge, one can then bioengineer a pathway aimed at more efficient hydrogen production.

In plants, it has been recently shown that FNR is physically anchored to the thylakoid membrane or to PSI (13) by direct binding (14) or through interaction with accessory proteins such as TROL (15), TIC82 (16), connectin (17), and other factors. It was reported that this association resulted in up to a 20-fold higher NADPH production rate compared to the rates catalyzed by soluble FNR (18) in vitro. Moreover, in the green algae *Chlamydomonas reinhardtii*, a model hydrogen-producing photosynthetic organism, both washed intact thylakoids (*SI Text*) and a PSI supercomplex from cells induced into CEF (19) (Fig. 1*B*) show the presence of FNR. Together, these observations led us to suggest that the localization of FNR to the thylakoids, near PSI, enables it to directly interact with PSI-reduced Fd, limiting electron transfer to competing processes such as hydrogen production. We examined the occurrence of this competition in vitro and investigated whether an Fd-HydA fusion is able to divert electron flow at PSI from Fd to FNR and NADPH production toward hydrogen production.

Results

Study of the Competition Between FNR and HydA for Reduced Fd.
To address the above questions, we prepared two in vitro reaction systems based on isolated thylakoids or purified PSI (Fig. 2). The thylakoid system consisted of either algal or plant thylakoid membranes, which allowed us to test whether the FNR activity known to be associated with thylakoid membranes from plants was also found in thylakoids from alga. It should be noted that, unlike plant thylakoids, exogenous plastocyanin (the natural electron donor to PSI) had to be added to the purified algal thylakoids because this protein was lost during preparation (see *SI Text*). The second in vitro system utilized purified PSI because, unlike thylakoids, these preparations lacked any detectable FNR activity. We observed that algal thylakoids, like the thylakoids from plants (see Fig. 2*C*), contained a membrane-associated FNR activity (*SI Text*), whereas the isolated PSI required the addition of exogenous FNR to actively photoproduce NADPH (*SI Text* and Fig. 2*C*).

We next investigated whether Fd preferentially interacts with membrane-bound FNR or with the soluble HydA by comparing the activities of both enzymes in vitro using each of the two experimental systems. We observed that addition of Fd supports hydrogen production by isolated thylakoids (in the absence of $NADP^+$) and purified PSI (with inactivated FNR and in the presence of $NADP^+$), whereas the addition of active FNR and $NADP^+$ inhibits hydrogen production by 75% or more in either system (Fig. 2*A*). This level of inhibition occurred in reactions with either thylakoids or purified PSI, suggesting that the level of competitive inhibition by FNR is similar, whether it is present in a membrane-bound FNR or added in a soluble form. It must be also noted that the thylakoid-catalyzed hydrogen production rates do not reach a maximum plateau under our experimental conditions, demonstrating that Fd is still the limiting factor, whereas PSI catalyzed hydrogen production was inhibited at Fd

concentrations above 10 μM. Addition of HydA to thylakoids at levels above 0.1 μM resulted in a gradual decrease in the rates of hydrogen production under noncompetitive conditions (Fig. 2*B*). This observation may be the result of protein aggregation (20) or a kinetic effect due to high HydA concentrations, leading to hydrogen oxidation and subsequent re-reduction of the Fd pool, which eventually increases the rates of NADPH production. Moreover, supplementation of thylakoids or PSI with active FNR and $NADP^+$ inhibited, but did not eliminate, hydrogen photoproduction at any of the HydA concentrations that were tested.

Addition of exogenous FNR to thylakoids had no effect on their NADPH production rate, indicating that the residual thylakoid-bound FNR was sufficient to saturate NADPH production kinetics (Fig. 2*C* and *SI Text*). The NADPH production catalyzed by PSI, as expected, is highly dependent on the concentration of added FNR, as observed above. The addition of up to a 10-fold higher concentration of HydA (100 nM) to the PSI or thylakoid reactions with a constant Fd concentration of 10 μM had no effect on the observed rates of NADPH production (Fig. 2*C*). This observation indicates that HydA was less efficient at interacting with Fd in the presence of FNR, possibly due to exogenous FNR forming a tight-binding complex with PSI as previously proposed (13). Interestingly, addition of 100 nM HydA had a stimulatory effect on FNR catalyzed NADPH production by thylakoids, most consistently at Fd concentrations above 15 μM (Fig. 2*D*). This stimulatory effect was initially observed by Abeles using crude unwashed *Chlamydomonas moewusii* thylakoids (21), which presumably contained both soluble and membrane-bound FNR. This phenomenon is possibly due to the recycling of hydrogen produced by high concentrations of HydA (see green plot, Fig. 2*B*) to Fd for conversion to NADPH by FNR. Finally, we show that Fd concentrations above 20 μM had a negative effect on the rates of NADPH production by thylakoids and isolated PSI, as reported by others (20) (Fig. 2*D*). In summary, it is clear that FNR interactions with PSI kinetically limits efficient electron transfer to HydA and hydrogen production.

Construction and Evaluation of Ferredoxin:Hydrogenase Fusion Proteins.
To bypass the dominating effect of FNR and give HydA a competitive advantage over FNR, we bioengineered, expressed and purified Fd-HydA fusion proteins. Our fusion protein approach was based on four key in vivo functions of Fd: (*i*) it is the sole electron donor to FNR for NADPH production, (*ii*) it mediates electron-transfer step from PSI to all outgoing metabolic processes, including CEF, (*iii*) it is a soluble protein that is not known to be physically associated with either thylakoids or other membrane components, and (*iv*) it forms a protein–protein electron-transfer complex directly with PSI. We postulated that a physical fusion between Fd and HydA would reduce the entropic contribution of the electron-transfer process among PSI, Fd, and HydA by restricting HydA to close proximity of PSI. In other words, PSI electrons will be shuttled directly through Fd to the tethered hydrogenase, kinetically limiting diversion of electrons to other competing metabolic pathways. To test the effect of HydA and Fd fusions on hydrogen photoproduction in vitro, we systematically designed and synthesized a series of Fd-HydA fusion proteins with linker lengths that varied from 10, 15, 20, 25, to 30 amino acids (aa) in increments of 5 aas, with both N-terminal and C-terminal Fd orientations. Each of the fusions consisted of the *C. reinhardtii hydA1* gene linked to the ferredoxin-1 (*petF*, and referred to here as Fd) gene by a linker peptide (Fig. 3*A*). All of the fusions were expressed in an *Escherichia coli* [FeFe]-hydrogenase maturation system (22). We were able to purify the fusions to homogeneity with a typical yield of 1.5 mg per liter of culture, at yields of approximately 40% (Fig. 3*B*). The fusion proteins showed a brownish color typical for FeS proteins, and UV-visible absorption features of Fe-S cluster and H-cluster charge-transfer bands (Fig. 3*C*).
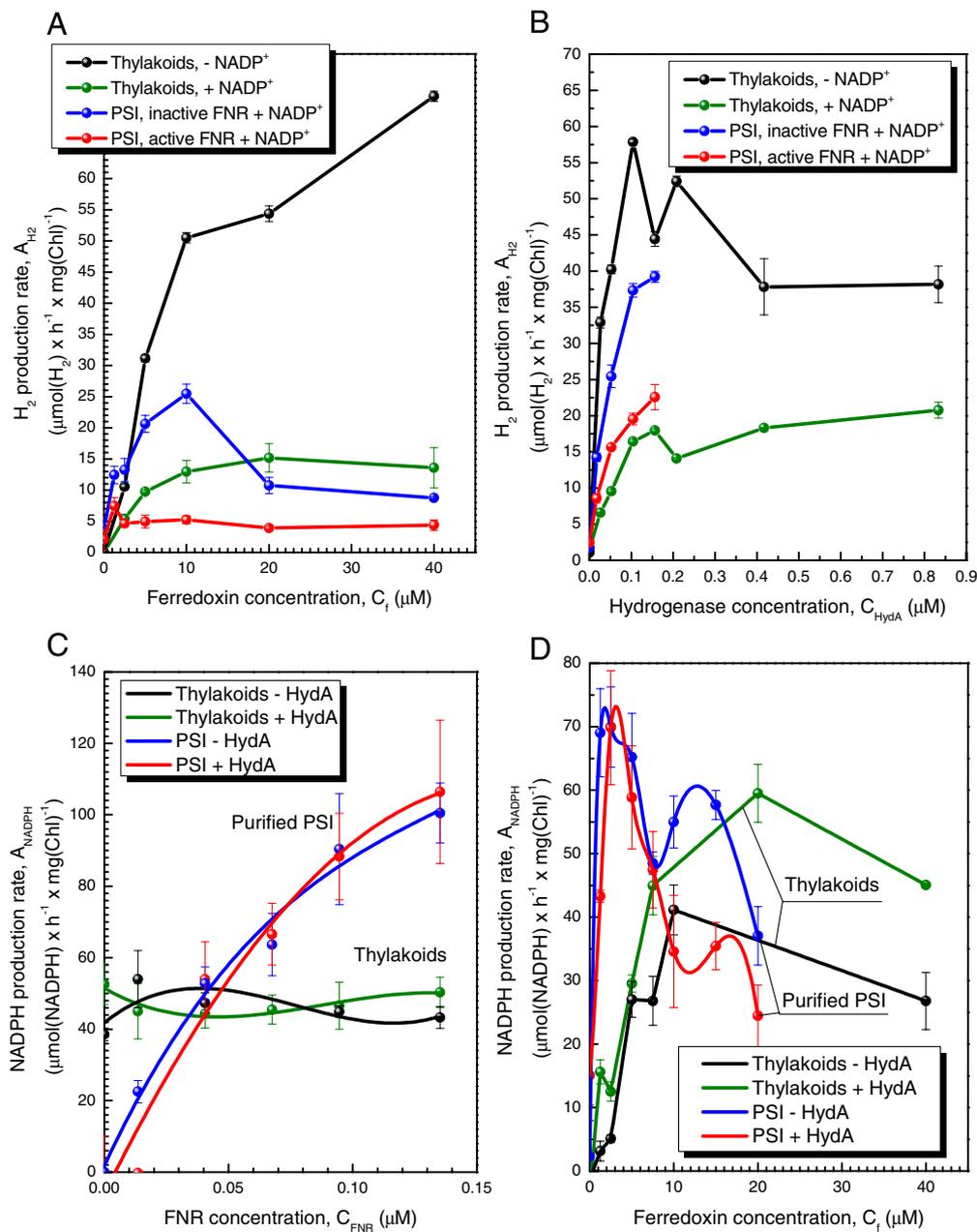
Fig. 2. *Kinetics of light-driven NADPH production versus hydrogen production.* Each of the in vitro reactions contained either plant thylakoids (25 µg chlorophyll, Chl) (black or green) or purified plant PSI (10 µg Chl) (blue and red) in combination with purified HydA and Fd to measure hydrogen production either in a noncompetitive reaction (the absence of $NADP^+$ for thylakoids, or with $NADP^+$ but heat inactivated FNR for PSI reactions) or competitive conditions (both active FNR and $NADP^+$). The competition between FNR and HydA for Fd was tested in reactions containing isolated thylakoids or purified PSI with varying concentrations of Fd (*A* and *D*), HydA (*B*), and FNR (*C*). (*A*) The rates of hydrogen production as a function of Fd concentration. HydA (100 nM) was incubated with (competitive) or without (noncompetitive) $NADP^+$ (2.5 mM) and active FNR (copurified with thylakoids, or added at 50 nM to purified PSI). Competition with NADPH production resulted in approximately 75% inhibition of hydrogen production at Fd concentrations higher than 5 µM with both thylakoids and PSI. (*B*) The rates of hydrogen production as a function of HydA concentration. HydA was added at increasing concentrations up to 850 nM for thylakoids or up to 200 nM for PSI as the concentrations above 100 nM are saturating. (*C*) The rates of NADPH production as a function of FNR concentration. The addition of external FNR to thylakoids did not alter the NADPH production rate, indicating this pathway is saturated by a membrane-associated FNR. The addition of HydA at a concentration of 100 nM, together with 10 µM Fd had no effect on either thylakoid or PSI mediated NADPH production rates. (*D*) The rates of NADPH production as a function of Fd concentration. FNR that either copurified with thylakoids or was exogenously added to PSI (50 nM) was combined in reactions Fd at up to 40 µM.

We first tested the activity of the purified Fd-HydA fusions in a hydrogen production reaction with the artificial electron donor, reduced methyl viologen (MV) (Fig. 3*B*). In this assay, Fd-HydA specific activities were as high as 3,000 U ($U = \mu mol\,H_2\,mg^{-1}\,min^{-1}$), compared to the 400 U for HydA (Fig. 3*B*). This enhanced activity was observed for both C- and N-terminal orientations of Fd. This result is similar to the activity enhancement effect observed for purified bacterial [FeFe]-hydrogenase from *Clostridium pasteurianum* when measured in the presence of both MV and reduced Fd, versus MV alone (23). Thus, the observed increases in MV activities for the Fd-HydA fusions is likely a result of HydA reduction by both MV and Fd, which results in the observed rate enhancement effect.

Effects of Fd-HydA Fusions on Photoproduction Rates of H_2 and NADPH. After evaluating fusion activities with the MV assay, we

assessed whether the fusions could function with PSI in a biochemical assay and enable photosynthetic light-driven hydrogen production. We measured the hydrogen production rate with purified PSI in the absence of free Fd. Under these reaction conditions, hydrogen photoproduction by HydA is negligible (less than $1\,\mu mol\,H_2\,mg\,Chl^{-1}\,h^{-1}$). Moreover, although the C-terminal HydA fusions (HydA-Fd) were biochemically active, they were inferior in the ability to catalyze the photoproduction of hydrogen. In contrast, we observed that the N-terminal Fd-15aa-HydA fusion photoproduced hydrogen at up to $10\,\mu mol\,H_2\,mg\,Chl^{-1}\,h^{-1}$ (*SI Text*). The hydrogen production rate was dependent on the length of the linker between Fd and HydA (Fig. 3*D*). The peak activity was observed for linkers consisting of 15–25 amino acids (Fig. 3*D*). When the Fd was fused to the HydA C terminus via a 10aa linker, the resulting fusion was not active; thus this HydA-Fd orientation was not used in further studies.
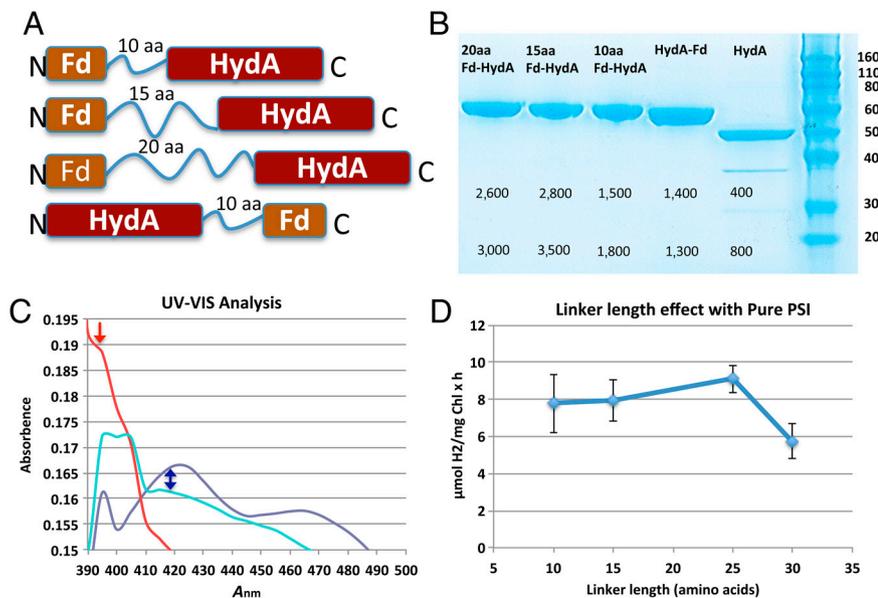
Fig. 3. Properties of the ferredoxin-hydrogenase fusion proteins. (A) Designs of fusion constructs showing the Fd and HydA orientations and aa linker lengths. Only 10–20 aa are shown. (B) SDS-PAGE of purified Fd-HydA fusions. Labels from right to left: protein size markers in kDa (Right); HydA, native C. reinhardtii HydA; HydA-Fd, a fusion of the HydA C terminus to the Fd N terminus with a 10-aa linker; Fd-HydA fusions of Fd C terminus to HydA N terminus with a 10-, 15-, or 20-aa linker (Left), respectively; only 10–20 aa are shown. The numbers below the protein bands represent the hydrogen production activities from the MV-sodium dithionite assay. Two values are shown for each enzyme, the specific activity in U units (Upper) and whole-cell activity (Lower) in units of nmol H_2 ml^{-1} min^{-1}. (C) UV-visible spectra of oxidized proteins, Fd (dark blue), HydA (red), and Fd-HydA (cyan). Fd shows a peak at approximately 421 nm, indicating the presence of the [2Fe-2S] cluster (marked by blue arrow). In contrast, HydA has a maximum at 395 nm (marked by red arrow) corresponding to the oxidized [6Fe-6S] H-cluster. The spectra of Fd-HydA show both a broader 395-nm peak of the H-cluster with a more intense 421-nm region that arises from the presence of the Fd [2Fe-2S] cluster. (D) The effect of linker length on the rate of hydrogen production in reactions with purified plant PSI and each of the Fd-HydA fusion proteins.

We then assessed the ability of the Fd-HydA to photoproduce hydrogen in direct competition with NADPH production using isolated thylakoids (Fig. 4). The N-terminal Fd fusion with the 15aa linker (Fd-15aa-HydA) was selected because there was little or no difference in the light-induced activities among fusions with linker lengths of 15, 20, or 25 amino acids (Fig. 3D).

We first measured photohydrogen production using purified PSI with varying concentrations of Fd-15aa-HydA with (Fig. 4A) or without externally added Fd (Fig. 4C). We found that the optimum working concentration for Fd-15aa-HydA was 1 μM (SI Text). Next, we challenged light-driven hydrogen production by Fd-15aa-HydA under two different reaction conditions with thylakoids. First, we tested the partitioning of reductant between Fd-15aa-HydA and FNR in the presence of NADP$^+$, but in the absence of Fd. Under these conditions, approximately 10% of electrons were diverted to NADPH, whereas approximately 90% were utilized for hydrogen production (Fig. 4C). This result shows that Fd-15aa-HydA competes with FNR and that the fused Fd mediates a direct interaction of Fd-15aa-HydA with PSI (referred to as mode 1 in Fig. 4 A and D), delivering a majority (90%) of the electrons to HydA for hydrogen production. A high partitioning of electrons to FNR (high NADPH production rates, and low hydrogen production rates) would indicate that Fd-15aa-HydA is inefficient at forming an electron-transfer complex at PSI. We also tested whether hydrogen production meditated by the Fd-15aa-HydA fusion could directly compete with the FNR that was associated with thylakoid membranes in the presence of free Fd and NADP$^+$ (Fig. 4A). We observed that Fd-15aa-HydA catalyzed rates of hydrogen photoproduction that were approximately 4-fold higher in magnitude compared to HydA at Fd concentrations of 10 μM (summarized in Table 1). Moreover, the diversion of PSI reductant to Fd-15aa-HydA allowed for simultaneous photoproduction of NADPH and hydrogen (mode 2, Fig. 4B) in reactions that contained Fd, and either purified PSI with free FNR, or thylakoids with intrinsic FNR (Table 1 and Fig. 4 A and B). Thus, substitution of HydA with Fd-15aa-HydA was shown to (i) catalyze H_2 production by two modes, a direct mode (1) and an indirect mode (2) involving Fd; (ii) decrease the NADPH production rates both in the presence and the absence of Fd; and (iii) abolish the stimulatory effect of H_2 production on

NADPH production that was observed in thylakoid reactions with HydA.

Discussion

In this work, we studied the competition of FNR and HydA for Fd with two in vitro systems: purified PSI and isolated thylakoids. We observed that FNR-mediated NADPH production limits the efficient hydrogen production by HydA in both systems. We present evidence that FNR is physically bound to the photosynthetic membrane in both plant and algal thylakoids. Moreover, our observations suggest that exogenous FNR is able to form a tight-binding complex with PSI, as previously proposed (13). However, these results might also be explained by the fact that lumenal and transmembrane features of purified PSI are exposed, which might result in artificial effects such as binding of FNR and/or HydA directly to PSI. We conclude that the presence of membrane or PSI bound FNR is the main factor inhibiting efficient electron transfer to soluble HydA, resulting in the low hydrogen production rates observed in vitro.

We were able to bypass the dominating effect of FNR by the design and application of a Fd-HydA fusion protein that functionally replaced HydA. The protein fusion strategy is a mature approach and has been successfully applied to several electron donors and acceptors (24–29). Indeed, a fusion between a bacterial [FeFe]-hydrogenase and Fd was recently reported (24). The reported fusion was designed to increase the efficiency of hydrogen production from glucose in bacterial cells. Glucose is another potential source for hydrogen production, but, in contrast with photohydrogen production, it requires an organic substrate and thus has much lower light conversion efficiency (additional photons are required to synthesize the sugar molecules fed to the bacteria). Moreover there are significant structural differences between algal and bacterial hydrogenases, which rendered contrasting results from those reported here, with the bacterial HydA-Fd fusion orientation being active in a fermentative pathway, whereas the Fd-HydA orientation was reported to be functionally inactive (24).

Our algal Fd-HydA fusion improved HydA function in several respects. First, the specific activities were up to sixfold higher than for the native HydA. Second, the fusion successfully insulates its internal Fd electrons, because only 10% of the electrons

Yacoby et al.
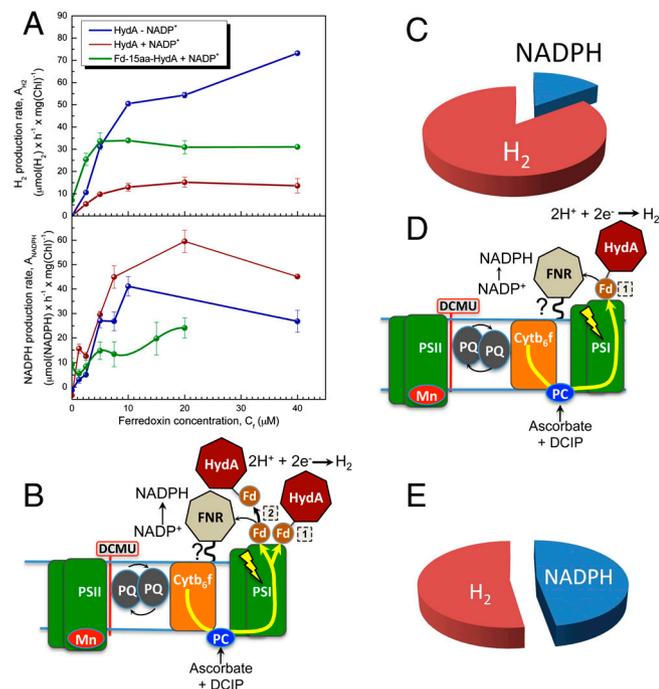
Fig. 4. *Competition for electrons between FNR and the fused Fd-15aa-HydA*. (*A*) Both hydrogen and NADPH production rates were measured under competitive and noncompetitive conditions. Each in vitro reaction contained plant thylakoids (25 μg chlorophyll, Chl) in combination with purified HydA (100 nM) or Fd-15aa-HydA (1 μM) and increasing concentrations of Fd up to 40 μM (x axis). Hydrogen production rates are shown (*Upper*) (noncompetitive, in the absence of NADP⁺; competitive, in the presence of NADP⁺). A significant increase in hydrogen production rates occurs under competitive conditions when HydA is replaced with Fd-15aa-HydA (brown versus green plots, respectively). NADPH production rates are shown (*Lower*) (noncompetitive, in the absence of HydA; competitive, in the presence of HydA or Fd-15aa-HydA). The NADPH production rates decrease, but are not completely inhibited, by the addition of Fd-15aa-HydA (green plot), whereas the rates increase with addition of HydA (brown plot) as observed before (see main text for discussion). This result strongly suggests that electrons are diverted at PS-I from FNR to Fd-15aa-HydA, resulting in increased hydrogen production rates but decreased NADPH production rates. (*D*) The schematic shows that, in the absence of free Fd, electrons generated at PSI during illumination are directly transferred to Fd-15aa-HydA (mode 1) and photohydrogen production. A small fraction (indicated by the small black arrow) of electrons are transferred from Fd of Fd-15aa-HydA to FNR for NADPH production. (*C*) The pie chart summarizes the data that are modeled in *D*. In the presence of Fd-15aa-HydA, and in the absence of free Fd, only approximately 10% of photosynthetic electrons are allocated to FNR and NADPH production and the remaining 90% to hydrogen production. (*B*) The schematic shows that both Fd-15aa-HydA (mode 1) and Fd (mode 2) are directly reduced at PSI to support hydrogen production, or simultaneous NADPH and hydrogen production (mode 2). The two electron-transfer modes at PSI allow for hydrogen production to compete with NADPH production. (*E*) The pie chart summarizes the results from *A* for 10 μM Fd, showing that Fd-15aa-HydA successfully competes with FNR to divert 60–70% of the electrons generated at PSI in thylakoids towards hydrogen production. In contrast, HydA not only catalyzes very low rates of hydrogen production in the presence of FNR, but also stimulates NADPH production rates (see also Fig. 4*A* and *SI Text*).

are lost to external competitors such as FNR. Third, the fusion was able to overcome FNR inhibition, as more than 60% of photosynthetic electrons were diverted to hydrogen production, compared to less than 10% for nonfused HydA.

In summary, we provide evidence that photosynthetic electron partitioning from hydrogen production is a result of thylakoid membrane and/or PSI-bound FNR. Moreover, we show that a Fd-HydA fusion can bypass this competition and result in more efficient photosynthetic hydrogen production. Although inhibition of hydrogen production at low carbon dioxide pressures

Table 1. Effect of the Fd-15aa-HydA fusion on the hydrogen production rates in PSI reactions under noncompetitive and competitive reaction conditions

Fd concentration, μM	Noncompetitive hydrogen production rate*		Competitive hydrogen production rate with NADP⁺ and FNR*	
	HydA	Fd-15aa-HydA	HydA	Fd-15aa-HydA
0	1	10	1	8
10	25	45	5	35

Noncompetitive, PSI (10 μg), HydA (0.1 μM) or Fd-15aa-HydA, (1 μM), PC (8 μM).

Competitive, same with addition of NADP⁺ (2.5 mM) FNR (0.1 μM).

*Rates are in units of $\mu mol\ H_2\ mg\ Chl^{-1}\ h^{-1}$.

in *C. reinhardtii* was previously studied in whole cells (9), the biochemical basis for this effect was not established. We clearly show that the NADPH production reaction catalyzed by FNR directly competes with hydrogen production by means of a physical association of FNR with either plant or algal thylakoid membranes. Moreover, a mechanism that involves a direct FNR:PSI association during electron transfer through Fd is also plausible, based on our results with purified PSI.

Furthermore, we have developed a previously undescribed approach that overcomes this competition between the two pathways and enhances hydrogen production in a photosynthetic process. Clearly our fusion approach has proven itself as a useful tool for accomplishing this goal and for further studying photosynthetic electron-transfer processes. Our observations could be used to develop strategies in order to control the distribution of photosynthetic power and enable feasible large-scale hydrogen production in the future.

Methods

Plasmid Construction. Plasmid constructs for the expression of *Chlamydomonas reinhardtii* [FeFe]-hydrogenases (HydA) in *E. coli* were developed from the pETDuet-based plasmids pHydEA and pHydFG as described (22). The modifications of pHydEA for the current study exchanged the *Chlamydomonas reinhardtii* HydA1 structural gene without any other alterations of HydE. The nucleotide sequence encoding the mature form of [FeFe]-hydrogenase HydA1 (Ala57-Lys497) of *C. reinhardtii* was fused to either the N or C terminus of the mature form of the *C. reinhardtii* ferredoxin (Ala32-Tyr126) petF (Fdx1, referred to here as Fd) with a 10 amino acid linker composed of Gly-Ser repeats (Thr-Gly-Gly-Gly-Ser-Gly-Gly-Gly-Ala-Ser). Please refer to *SI Text* for more details.

Protein Purification Expression. Protein purification expression was done as described (22) with few modifications; see supplementary information *SI Text* for detailed protocol.

Protein Gel Electrophoresis. Protein gel electrophoresis was performed with Invitrogen NuPAGE® Novex® Bis-Tris Gel Systems according to manufacturer instructions.

Purification of Plastocyanin. Plastocyanin (PC) was purified from pea leaves during the process of PSI isolation (30). See *SI Text* for details.

Hydrogen Production by Solubilized *E. coli* Whole Cells Expressing Recombinant Hydrogenase. Hydrogenase activity in whole cells was measured as described (22) with some modifications. See *SI Text* for more details.

Hydrogen Photoproduction by Thylakoids. Thylakoids were prepared from either *C. reinhardtii*, deveined pea, Swiss chard leaves, or spinach as described (30). See more details in *SI Text*. Reactions were prepared in 13-mL serum vials. A 0.9-mL volume of buffer A (*SI Text*) was added to the vial, 2 μL of 3-(3,4-dichlorophenyl)-1,1-dimethylurea (DCMU) (0.3 mM), 5 μL of dichloroindophenol (DCIP) (100 μM) and 10 μL of sodium ascorbate (SAsc) (1 M) were added. After that, 10 μL of glucose oxidase (30 mg mL⁻¹), 10 μL of glucose

(5 M), 10 μL of catalase (10 mg mL^{-1}), and 50 μL of ethanol 96% has been added to the reaction mixture. Then, the desired amount of Fd and FNR was added. For *Chlamydomonas* thylakoids, 30 μL of PC at 3 mg mL^{-1} was added because, unlike in higher plants, PC is lost during thylakoid preparation. All thylakoid isolation steps were performed in the dark. The amount of thylakoids used in all the hydrogen production reactions was measured as a chlorophyll concentration of 25 μg mL^{-1}. See *SI Text* for more details.

Hydrogen Photoproduction by PSI. Hydrogen photoproduction by PSI was done similarly to plant thylakoids with few modification; see *SI Text*.

NADPH Photoproduction. Buffer A (0.9 mL, *SI Text*) was added to a 1-mL cuvette with 2 μL of DCMU, 5 μL of DCIP, and 10 μL of SAsc. After mixing, 10–40 μL of a 3 mg mL^{-1} stock of PC was added, followed by different amounts of Fd, HydA, and FNR. Purified thylakoids or PSI was added to the solution in the dark. After mixing, 50 μL of NADP$^+$ was added and the cuvette was sealed with parafilm. The reaction was performed using halogen lamp as a light source. The concentration of NADPH was read every 30 s as a change of absorbance at 340 nm. A UV-visible spectrometer Beckman DU530 was used for absorbance measurement. The NADP$^+$ reduction rate (μmol NADPH mg Chl^{-1} h^{-1}) was calculated according to the equation

$$\text{rate} = A_{340}/6.22 \times (1/\text{Chl}_{\text{mg mL}^{-1}}/T_s \times 3{,}600_{\text{s h}^{-1}}),$$

where A_{340} is the optical absorption at 340 nm, 6.22 is the NADPH extinction coefficient (mM^{-1}), Chl$_{\text{mg/mL}}$ is the concentration of chlorophyll, and T_s is the illumination time.

1. Gaffron H, Rubin J (1942) Fermentative and photochemical production of hydrogen in algae. *J Gen Physiol* 26:219–240.
2. Melis A, Happe T (2004) Trails of green alga hydrogen research—From hans gaffron to new frontiers. *Photosynth Res* 80:401–409.
3. Happe T, Hemschemeier A, Winkler M, Kaminski A (2002) Hydrogenases in green algae: Do they save the algae's life and solve our energy problems? *Trends Plant Sci* 7:246–250.
4. Ghirardi ML, et al. (2007) Hydrogenases and hydrogen photoproduction in oxygenic photosynthetic organisms. *Annu Rev Plant Biol* 58:71–91.
5. Nelson N, Yocum CF (2006) Structure and function of photosystems I and II. *Annu Rev Plant Biol* 57:521–565.
6. Terauchi AM, et al. (2009) Pattern of expression and substrate specificity of chloroplast ferredoxins from Chlamydomonas reinhardtii. *J Biol Chem* 284:25867–25878.
7. Hemschemeier A, Fouchard S, Cournac L, Peltier G, Happe T (2007) Hydrogen production by Chlamydomonas reinhardtii: An elaborate interplay of electron sources and sinks. *Planta* 227:397–407.
8. Kruse O, et al. (2005) Improved photobiological H2 production in engineered green algal cells. *J Biol Chem* 280:34170–34177.
9. Cinco RM, MacInnis JM, Greenbaum E (1993) The role of carbon dioxide in light-activated hydrogen production by Chlamydomonas reinhardtii. *Photosynth Res* 38:27–33.
10. Melis A, Zhang L, Forestier M, Ghirardi ML, Seibert M (2000) Sustained photobiological hydrogen gas production upon reversible inactivation of oxygen evolution in the green alga Chlamydomonas reinhardtii. *Plant Physiol* 122:127–136.
11. Giannelli L, Scoma A, Torzillo G (2009) Interplay between light intensity, chlorophyll concentration and culture mixing on the hydrogen production in sulfur-deprived Chlamydomonas reinhardtii cultures grown in laboratory photobioreactors. *Biotechnol Bioeng* 104:76–90.
12. Lien S, Pietro AS (1981) Effect of uncouplers on anaerobic adaptation of hydrogenase activity in. *Biochem Biophys Res Commun* 103:139–147.
13. van Thor JJ, Geerlings TH, Matthijs HC, Hellingwerf KJ (1999) Kinetic evidence for the PsaE-dependent transient ternary complex photosystem I/Ferredoxin/Ferredoxin: NADP(+) reductase in a cyanobacterium. *Biochemistry* 38:12735–12746.
14. Grzyb J, Gagos M, Gruszecki WI, Bojko M, Strzalka K (2008) Interaction of ferredoxin: NADP+ oxidoreductase with model membranes. *Biochim Biophys Acta* 1778:133–142.
15. Juric S, et al. (2009) Tethering of ferredoxin:NADP+ oxidoreductase to thylakoid membranes is mediated by novel chloroplast protein TROL. *Plant J* 60:783–794.
16. Benz JP, et al. (2009) Arabidopsis Tic62 and ferredoxin-NADP(H) oxidoreductase form light-regulated complexes that are integrated into the chloroplast redox poise. *Plant Cell* 21:3965–3983.
17. Shin M (2004) How is ferredoxin-NADP reductase involved in the NADP photoreduction of chloroplasts? *Photosynth Res* 80:307–313.
18. Forti G, Bracale M (1984) Ferredoxin–ferredoxin NADP reductase interaction: Catalytic differences between the soluble and thylakoid-bound complex. *FEBS Lett* 166:81–84.
19. Iwai M, et al. (2010) Isolation of the elusive supercomplex that drives cyclic electron flow in photosynthesis. *Nature* 464:1210–1213.
20. Fourmond V, Lagoutte B, Setif P, Leibl W, Demaille C (2007) Electrochemical study of a reconstituted photosynthetic electron-transfer chain. *J Am Chem Soc* 129:9201–9209.
21. Abeles FB (1964) Cell-free hydrogenase from Chlamydomonas. *Plant Physiol* 39:169–176.
22. King PW, Posewitz MC, Ghirardi ML, Seibert M (2006) Functional studies of [FeFe] hydrogenase maturation in an Escherichia coli biosynthetic system. *J Bacteriol* 188:2163–2172.
23. Chen J-S, Mortenson LE (1974) Purification and properties of hydrogenase from Clostridium pasteurianum W5. *Biochim Biophys Acta* 371:283–298.
24. Agapakis CM, et al. (2010) Insulation of a synthetic hydrogen metabolism circuit in bacteria. *J Biol Eng* 4:1–15.
25. Aliverti A, Zanetti G (1997) A three-domain iron-sulfur flavoprotein obtained through gene fusion of ferredoxin and ferredoxin-NADP+ reductase from spinach leaves. *Biochemistry* 36:14771–14777.
26. Blazyk JL, Lippard SJ (2003) Domain engineering of the reductase component of soluble methane monooxygenase from Methylococcus capsulatus (Bath). *J Biol Chem* 279:5630–5640.
27. Kimata-Ariga Y, Sakakibara Y, Ikegami T, Hase T (2010) Electron transfer of site-specifically cross-linked complexes between ferredoxin and ferredoxin-NADP$^+$ reductase. *Biochemistry* 49:10013–10023.
28. Lacour T, Ohkawa H (1999) Engineering and biochemical characterization of the rat microsomal cytochrome P4501A1 fused to ferredoxin and ferredoxin-NADP(+) reductase from plant chloroplasts. *Biochim Biophys Acta* 1433:87–102.
29. Zanetti G, Piubelli L, Zucca Tanci R, Aliverti A (1996) A chimeric iron-sulfur flavoprotein endowed with NADPH-cytochrome c reductase activity. *Biochem Soc Trans* 24:22S.
30. Amunts A, Toporik H, Borovikova A, Nelson N (2010) Structure determination and improved model of plant photosystem I. *J Biol Chem* 285(5):3478–3486.

Yacoby et al.